Low loss Ge-As-Se chalcogenide glass fiber, fabricated using extruded preform, for mid-infrared photonics

Zhuoqi Tang,[1] Vladimir S. Shiryaev,[2] David Furniss,[1] Lukasz Sojka,[1] Slawomir Sujecki,[1] Trevor M. Benson,[1] Angela B. Seddon[1]* and Mikhail F. Churbanov[2]

[1]*Mid-Infrared Photonics Group, George Green Institute for Electromagnetics Research, Faculty of Engineering, University of Nottingham, University Park, Nottingham NG7 2RD, UK*

[2]*Institute of Chemistry of High-Purity Substances of the Russian Academy of Sciences, 49 Tropinin Str., Nizhny Novgorod 603950, Russia*

**angela.seddon@nottingham.ac.uk*

Abstract: Chalcogenide glass fibers have attractive properties (e.g. wide transparent window, high optical non-linearity) and numerous potential applications in the mid-infrared (MIR) region. Low optical loss is desired and important in the development of these fibers. Ge-As-Se glass has a large glass-forming range to provide versatility of choice from continuously varying physical properties. Recently, broadband MIR supercontinuum generation has been achieved in chalcogenide fibers by using Ge-As-Se glass in the core/clad. structure. In the shaping of chalcogenide glass optical fiber preforms, extrusion is a useful technique. This work reports glass properties (viscosity-temperature curve and glass transition) and optical losses of Ge-As-Se fiber fabricated from an extruded preform. A robust cut-back method of fiber loss measurement is developed and the corresponding error calculation discussed. MIR light is propagated through 52 meters of a fiber, which has the lowest loss yet reported for Ge-As-Se fiber of 83 ± 2 dB/km at 6.60 μm wavelength. The fiber baseline loss is 83-90 dB/km across 5.6-6.8 μm, a Se-H impurity absorption band of 1.4 dB/m at 4.5 μm wavelength is superposed and other impurity bands (e.g. O-H, As-O, Ge-O) are ≤ 20 dB/km. Optical losses of fiber fabricated from different positions of the extruded preform are investigated.

OCIS codes: (060.2390) Fiber optics, infrared; (060.2270) Fiber characterization; (060.2290) Fiber materials.

References and links

1. B. J. Eggleton, "Chalcogenide photonics: fabrication, devices and applications introduction," Opt. Express **18**(25), 26632–26634 (2010).
2. G. E. Snopatin, M. F. Churbanov, A. A. Pushkin, V. V. Gerasimenko, E. M. Dianov, and V. G. Plotnichenko, "High purity arsenic-sulfide glasses and fibers with minimum attenuation of 12 dB/km," Optoelectron Adv. Mat. **3**(7), 669–671 (2009).
3. J. S. Sanghera, L. B. Shaw, and I. D. Aggarwal, "Chalcogenide glass-fiber-based mid-IR sources and applications," IEEE J. Quantum Electron. **15**(1), 114–119 (2009).
4. A. B. Seddon, Z. Tang, D. Furniss, S. Sujecki, and T. M. Benson, "Progress in rare-earth-doped mid-infrared fiber lasers," Opt. Express **18**(25), 26704–26719 (2010).
5. C. R. Petersen, U. Møller, I. Kubat, B. Zhou, S. Dupont, J. Ramsay, T. Benson, S. Sujecki, N. Abdel-Moneim, Z. Tang, D. Furniss, A. Seddon, and O. Bang, "Mid-infrared supercontinuum covering the 1.4–13.3 μm molecular fingerprint region using ultra-high NA chalcogenide step-index fibre," Nat. Photonics **8**(11), 830–834 (2014).
6. J. S. Sanghera and I. D. Aggarwal, "Active and passive chalcogenide glass optical fibers for IR applications: a review," J. Non-Cryst. Solids **256–257**(0), 6–16 (1999).
7. M. Churbanov, G. Snopatin, V. Shiryaev, V. Plotnichenko, and E. Dianov, "Recent advances in preparation of high-purity glasses based on arsenic chalcogenides for fiber optics," J. Non-Cryst. Solids **357**(11), 2352–2357 (2011).

#239909 Received 28 Apr 2015; revised 22 May 2015; accepted 15 Jun 2015; published 7 Jul 2015

8. V. Q. Nguyen, J. S. Sanghera, P. Pureza, F. H. Kung, and I. D. Aggarwal, "Fabrication of arsenic selenide optical fiber with low hydrogen impurities," J. Am. Ceram. Soc. **85**(11), 2849–2851 (2002).
9. A. Zakery and S. Elliott, "Optical properties and applications of chalcogenide glasses: a review," J. Non-Cryst. Solids **330**(1), 1–12 (2003).
10. A. B. Seddon, "Chalcogenide glasses: a review of their preparation, properties and applications," J. Non-Cryst. Solids **184**(0), 44–50 (1995).
11. Z. Tang, D. Furniss, M. Fay, N. C. Neate, Y. Cheng, E. Barney, L. Sojka, S. Sujecki, T. M. Benson, and A. B. Seddon, "First identification of rare-earth oxide nucleation in chalcogenide glasses and implications for fabrication of mid-infrared active fibers," J. Am. Ceram. Soc. **97**(2), 432–441 (2014).
12. G. E. Snopatin, V. S. Shiryaev, V. G. Plotnichenko, E. M. Dianov, and M. F. Churbanov, "High-purity chalcogenide glasses for fiber optics," Inorg. Mater. **45**(13), 1439–1460 (2009).
13. B. J. Eggleton, B. Luther-Davies, and K. Richardson, "Chalcogenide photonics," Nat. Photonics **5**(3), 141–148 (2011).
14. T. Katsuyama, K. Ishida, S. Satoh, and H. Matsumura, "Low loss Ge-Se chalcogenide glass optical fibers," Appl. Phys. Lett. **45**(9), 925–927 (1984).
15. M. F. Churbanov, I. V. Scripachev, G. E. Snopatin, V. S. Shiryaev, and V. G. Plotnichenko, "High-purity glasses based on arsenic chalcogenides," J. Optoelectron. Adv. Mater. **3**(2), 341–349 (2001).
16. H. Xu, Y. He, X. Wang, Q. Nie, P. Zhang, T. Xu, S. Dai, X. Zhang, and G. Tao, "Preparation of low-loss $Ge_{15}Ga_{10}Te_{75}$ chalcogenide glass for far-IR optics applications," Infrared Phys. Technol. **65**(0), 77–82 (2014).
17. J. Troles, V. Shiryaev, M. Churbanov, P. Houizot, L. Brilland, F. Desevedavy, F. Charpentier, T. Pain, G. Snopatin, and J. L. Adam, "$GeSe_4$ glass fibres with low optical losses in the mid-IR," Opt. Mater. **32**(1), 212–215 (2009).
18. V. S. Shiryaev, J. L. Adam, X. H. Zhang, C. Boussard-Plédel, J. Lucas, and M. F. Churbanov, "Infrared fibers based on Te–As–Se glass system with low optical losses," J. Non-Cryst. Solids **336**(2), 113–119 (2004).
19. E. M. Dianov, M. Y. Petrov, V. G. e. Plotnichenko, and V. K. Sysoev, "Estimate of the minimum optical losses in chalcogenide glasses," Quantum Electron. **12**(4), 498–499 (1982).
20. J. S. Sanghera and I. D. Aggarwal, "Development of chalcogenide glass fiber optics at NRL," J. Non-Cryst. Solids **213–214**(0), 63–67 (1997).
21. G. G. Devyatykh, E. M. Dianov, V. G. Plotnichenko, I. V. Skripachev, and M. F. Churbanov, "Fiber waveguides based on high-purity chalcogenide glasses," High-Purity Substances **5**(1), 1–27 (1991).
22. F. Désévédavy, G. Renversez, L. Brilland, P. Houizot, J. Troles, Q. Coulombier, F. Smektala, N. Traynor, and J.-L. Adam, "Small-core chalcogenide microstructured fibers for the infrared," Appl. Opt. **47**(32), 6014–6021 (2008).
23. M. F. Churbanov, V. S. Shiryaev, A. I. Suchkov, A. A. Pushkin, V. V. Gerasimenko, R. M. Shaposhnikov, E. M. Dianov, V. G. Plotnichenko, V. V. Koltashev, Y. N. Pyrkov, J. Lucas, and J. L. Adam, "High-purity As-S-Se and As-Se-Te glasses and optical fibers," Inorg. Mater. **43**(4), 441–447 (2007).
24. J. Troles, Y. Niu, C. Duverger-Arfuso, F. Smektala, L. Brilland, V. Nazabal, V. Moizan, F. Desevedavy, and P. Houizot, "Synthesis and characterization of chalcogenide glasses from the system Ga–Ge–Sb–S and preparation of a single-mode fiber at 1.55 μm," Mater. Res. Bull. **43**(4), 976–982 (2008).
25. J. S. Sanghera, V. Q. Nguyen, P. C. Pureza, F. H. Kung, R. Miklos, and I. D. Aggarwal, "Fabrication of low-loss IR-transmitting $Ge_{30}As_{10}Se_{30}Te_{30}$ glass fibers," Lightwave Technology, Journalism **12**(5), 737–741 (1994).
26. P. Toupin, L. Brilland, J. Trolès, and J.-L. Adam, "Small core Ge-As-Se microstructured optical fiber with single-mode propagation and low optical losses," Opt. Mater. Express **2**(10), 1359–1366 (2012).
27. Z. Lian, Q. Li, D. Furniss, T. M. Benson, and A. B. Seddon, "Solid microstructured chalcogenide glass optical fibers for the near- and mid-infrared spectral regions," Photonics Technology Letters, IEEE **21**(24), 1804–1806 (2009).
28. Y. Yu, B. Zhang, X. Gai, C. Zhai, S. Qi, W. Guo, Z. Yang, R. Wang, D.-Y. Choi, S. Madden, and B. Luther-Davies, "1.8-10 μm mid-infrared supercontinuum generated in a step-index chalcogenide fiber using low peak pump power," Opt. Lett. **40**(6), 1081–1084 (2015).
29. B. Zhang, W. Guo, Y. Yu, C. Zhai, S. Qi, A. Yang, L. Li, Z. Yang, R. Wang, and D. Tang, "Low loss, high NA chalcogenide glass fibers for broadband mid-Infrared supercontinuum generation," J. Am. Ceram. Soc. **98**(5), 1389–1392 (2015).
30. I. Kubat, C. S. Agger, U. Møller, A. B. Seddon, Z. Tang, S. Sujecki, T. M. Benson, D. Furniss, S. Lamrini, K. Scholle, P. Fuhrberg, B. Napier, M. Farries, J. Ward, P. M. Moselund, and O. Bang, "Mid-infrared supercontinuum generation to 12.5μm in large NA chalcogenide step-index fibres pumped at 4.5μm," Opt. Express **22**(16), 19169–19182 (2014).
31. T. Kanamori, Y. Terunuma, S. Takahashi, and T. Miyashita, "Chalcogenide glass fibers for mid-infrared transmission," J. Lightwave Technol. **2**(5), 607–613 (1984).
32. I. V. Scripachev, M. F. Churbanov, V. V. Gerasimenko, G. E. Snopatin, V. S. Shiryaev, A. A. Pushkin, I. E. Fadin, V. G. Plotnichenko, and Y. N. Pyrkov, "Optical and mechanical characteristics of fibers made of arsenic chalcogenides," J. Optoelectron. Adv. Mater. **3**(2), 351–360 (2001).
33. E. Roeder, "Flow behaviour of glass during extrusion," J. Non-Cryst. Solids **7**(2), 203–220 (1972).
34. D. Furniss and A. B. Seddon, "Towards monomode proportioned fibreoptic preforms by extrusion," J. Non-Cryst. Solids **256**, 232–236 (1999).

#239909 Received 28 Apr 2015; revised 22 May 2015; accepted 15 Jun 2015; published 7 Jul 2015

35. S. D. Savage, C. A. Miller, D. Furniss, and A. B. Seddon, "Extrusion of chalcogenide glass preforms and drawing to multimode optical fibers," J. Non-Cryst. Solids **354**(29), 3418–3427 (2008).
36. D. J. Gibson and J. A. Harrington, "Extrusion of hollow waveguide preforms with a one-dimensional photonic bandgap structure," J. Appl. Phys. **95**(8), 3895–3900 (2004).
37. K. Bhowmick, H. P. Morvan, D. Furniss, A. B. Seddon, and T. M. Benson, "Co-extrusion of multilayer glass fiber-optic preforms: prediction of layer dimensions in the extrudate," J. Am. Ceram. Soc. **96**(1), 118–124 (2013).
38. G. Tao, S. Shabahang, S. Dai, and A. F. Abouraddy, "Multimaterial disc-to-fiber approach to efficiently produce robust infrared fibers," Opt. Mater. Express **4**(10), 2143–2149 (2014).
39. G. Tao, S. Shabahang, E.-H. Banaei, J. J. Kaufman, and A. F. Abouraddy, "Multimaterial preform coextrusion for robust chalcogenide optical fibers and tapers," Opt. Lett. **37**(13), 2751–2753 (2012).
40. Z. Tang, D. Furniss, M. Fay, H. Sakr, L. Sójka, N. Neate, N. Weston, S. Sujecki, T. M. Benson, and A. B. Seddon, "Mid-infrared photoluminescence in small-core fiber of praseodymium-ion doped selenide-based chalcogenide glass," Opt. Mater. Express **5**(4), 870–886 (2015).
41. A. N. Gent, "Theory of the parallel plate viscometer," Br. J. Appl. Phys. **11**(2), 85–87 (1960).
42. V. S. Shiryaev, M. F. Churbanov, E. M. Dianov, V. G. Plotnichenko, J. L. Adam, and J. Lucas, "Recent progress in preparation of chalcogenide As-Se-Te glasses with low impurity content," J. Optoelectron. Adv. Mater. **7**(4), 1773–1779 (2005).
43. G. G. Devyatykh, M. F. Churbanov, I. V. Scripachev, G. E. Snopatin, E. M. Dianov, and V. G. Plotnichenko, "Recent developments in As–S glass fibres," J. Non-Cryst. Solids **256–257**(0), 318–322 (1999).
44. M. F. Churbanov, V. S. Shiryaev, V. V. Gerasimenko, A. A. Pushkin, I. V. Skripachev, G. E. Snopatin, and V. G. Plotnichenko, "Stability of the optical and mechanical properties of chalcogenide fibers," Inorg. Mater. **38**(10), 1063–1068 (2002).
45. Y. Cheng, Z. Tang, N. C. Neate, D. Furniss, T. M. Benson, and A. B. Seddon, "The influence of dysprosium addition on the crystallization behavior of a chalcogenide selenide glass close to the fiber drawing temperature," J. Am. Ceram. Soc. **95**(12), 3834–3841 (2012).
46. W. A. King, A. G. Clare, and W. C. Lacourse, "Laboratory preparation of highly pure As_2Se_3 glass," J. Non-Cryst. Solids **181**(3), 231–237 (1995).
47. A. M. Reitter, A. N. Sreeram, A. K. Varshneya, and D. R. Swiler, "Modified preparation procedure for laboratory melting of multicomponent chalcogenide glasses," J. Non-Cryst. Solids **139**, 121–128 (1992).
48. M. Churbanov, "High-purity chalcogenide glasses as materials for fiber optics," J. Non-Cryst. Solids **184**, 25–29 (1995).
49. M. Maklad, R. Mohr, R. Howard, P. Macedo, and C. Moynihan, "Multiphonon absorption in As_2S_3-As_2Se_3 glasses," Solid State Commun. **15**(5), 855–858 (1974).
50. Z. Tang, N. C. Neate, D. Furniss, S. Sujecki, T. M. Benson, and A. B. Seddon, "Crystallization behavior of Dy^{3+}-doped selenide glasses," J. Non-Cryst. Solids **357**(11–13), 2453–2462 (2011).

1. Introduction

Chalcogenide glasses (based on S, Se, and Te) have been studied for more than 60 years [1]. They have shown attractive properties including a wide transparency range from the visible to the mid-infrared (MIR), chemical durability, high optical non-linearity, ability to be drawn into fiber [2–4] and wide supercontinuum (SC) generation in fiber [5]. Based on these properties, chalcogenide glass fibers present numerous potential applications in the MIR spectral region, like medical diagnostics, laser power delivery, bio- and chemical sensing, imaging, near-field microscopy and non-linear optical systems [1, 6–11].

In the progress of development and application of chalcogenide optical fibers, lowering the impurity content in the glasses has always been of concern in order to minimize extrinsic optical loss [12]. Glass purity is one of the most important issues in achieving maximum utility of chalcogenide glass fibers [13] and research on low optical loss chalcogenide glass fiber has been carried out for more than 30 years [14]. Impurities, including hydrogen-based, oxygen-based, carbon-based, metallic and SiO_2, have impeded improving the purity of chalcogenide glass fiber [7, 15]. The distillation technique [16–18] is one of the most important paths to low loss chalcogenide glass fiber. Especially, O-getters (*e.g.* Al, Mg) and H-getters (e.g. $TeCl_4$) can be applied in the distillation to reduce H and O related impurities (*viz.*: -O-H, H_2O, -Se-H, -S-H, = As-O- and ≡Ge-O-]. For example, in 2002, Nguyen *et al.* applied a vacuum distillation with Al and $TeCl_4$ getters to achieve a low 0.2 dB/m Se-H impurity band in an As-Se core/clad. fiber [8]. Also, a double vacuum distillation with an Al getter was used to achieve a minimum optical loss of 40 dB/km at 6.7 μm wavelength in a Te-As-Se unclad fiber, reported by Shiryaev *et al.* in 2004 [18].

#239909 Received 28 Apr 2015; revised 22 May 2015; accepted 15 Jun 2015; published 7 Jul 2015

Generally, reports of the lowest loss of chalcogenide glass fiber are in the region of 50-300 dB/km across the 2-9 μm wavelength range [12]. The world champion loss of chalcogenide glass fiber remains 12 dB/km at 3.0 μm in an As-S core/clad. fiber, reported by Snopatin *et al.* in 2009 [2]; they referred to the theoretical minimum loss of As-S as 0.05 dB/km at 4.3 μm wavelength [19]. Compare this with another estimated theoretical minimum loss of As-S glass, of 4 dB/km at 5.0 μm wavelength, when the weak absorption tail was considered [20]. Table 1 summarizes the typical ultra-low loss data reported to date for chalcogenide glass fiber of various elemental systems. Normally, as the glass system incorporates more elements, low loss is more difficult to achieve. Also, within the same glass system, core/clad. fiber can present higher loss than unclad. fiber because defects (*e.g.* bubbles, geometrical imperfections) or crystallization can be introduced at the core/clad. interface, increasing the extrinsic scattering loss. Table 1 shows that the minimum ultra-low loss currently achievable in chalcogenide glass fiber is between ~10-110 dB/km, depending on the glass system.

Table 1. Typical ultra-low loss data for chalcogenide glass fiber based on different elemental systems.

Glass system	Fiber structure	Minimum loss / (dB/km)	Wavelength / (μm)	Reference
		Two element systems		
As-S	core/clad.	12	3.0	[2]
As-Se	unclad.	76	4.0	[21]
Ge-Se	unclad.	100	6.6	[17]
		Three element systems		
As-Se-Te	unclad.	40	6.7	[18]
Ge-Sb-S	unclad.	50	2.3	[22]
As-Se-S	core/clad.	60	4.8	[23]
Ge-As-Se	unclad.	83	6.6	This work
		Four element systems		
Ge-Sb-Ga-S	unclad.	100	2.8	[24]
Ge-As-Se-Te	unclad.	110	6.6	[25]

In this work, we concentrate on the Ge-As-Se glass system which has an exceptionally large glass-forming range [13]. Ge-As-Se glass has been applied in the core [26] or clad [27]. of chalcogenide glass structured optical fibers. Recently (2014-2015), extreme broadband MIR supercontinuum (SC) generation has been demonstrated in chalcogenide glass fibers [5], and Ge-As-Se glass was designed as the core [28, 29] or clad [5, 30]. in these fibers which were optically engineered to have high numerical aperture (NA). Thus, we have successfully modelled [30] and fabricated [5] NA = 1 fibers by using Ge-As-Se glass as the clad. to achieve record MIR SC from 1.4 to 13.3 μm.

The (minimum) optical losses of unclad Ge-As-Se fibers have been reported variously as 182 dB/km at 2.12 μm wavelength [31], 280 dB/km at 6.8 μm wavelength [12], 90-300 dB/km across the 2-6 μm wavelength range [32] and below 1 dB/m in 1.5-9 μm wavelength region [26]. In this work, we report the lowest minimum loss, to our knowledge, of unclad Ge-As-Se fiber as 83 ± 2 dB/km at 6.60 μm wavelength.

In chalcogenide glass shaping, extrusion is a particularly flexible technique for the manufacture of rods, tubes and other arbitrary profiles [27, 33, 34]. Supercooled glass-melt stability, to avoid crystallization, is required during extrusion because it is a re-heat-treatment process that can take a few hours. Extrusion can help achieve low interfacial roughness (*i.e.* lower scattering loss) in the fabrication of step-index chalcogenide glass fiber [35] and extrusion of chalcogenide glass for fiberoptic preform fabrication has been investigated in several publications [35–39]. In 2008, we reported [35] the co-extrusion of Ge-As-Se/Ge-As-

#239909 Received 28 Apr 2015; revised 22 May 2015; accepted 15 Jun 2015; published 7 Jul 2015

Se-S core/clad. fiber with a minimum fiber loss of 1.6 dB/m at 6.0 μm wavelength. Due to the supercooled glass-melt behavior (*e.g.* crystallization behavior), and impurities which can be introduced during the extrusion (*e.g.* bubbles), different positions of the extruded preform can produce fibers of differing loss. Thus, this work will explore the low loss fiber status and the fiber stability/quality when drawn from different positions of the extruded preform.

The fiber cut-back approach has been widely used for measuring the optical loss of chalcogenide glass fibers [2, 23–25, 40]. Based on the standard cut-back method, but with the aim of achieving more reliable loss results for these low Young's modulus, non-silica glasses, a robust fiber loss measurement method has been developed here together with a method of loss-error calculation and these are discussed in detail in this work. Finally, viscosity-temperature and differential scanning calorimetry (DSC) curves of the Ge-As-Ga glass are reported with a discussion of how the methodology adopted was optimized.

2. Experimental

2.1 Glass and fiber preparation

Ge (5N purity, Materion), As (7N5 purity, Furakawa Denshi; prior heat treated at 310°C under vacuum (10^{-3} Pa)) and Se (5N purity, Materion; prior heat treated at 270°C under vacuum (10^{-3} Pa)) were batched in a silica glass ampoule and melted at 850°C for 20 hours, air quenched to around the glass transition temperature (T_g, *i.e.* 160°C) and annealed at T_g for 1 hour and finally cooled down to ambient temperature to form a $Ge_{10}As_{21}Se_{69}$ (atomic% (at%)) glass, which was then used for the glass characterization of viscosity-temperature and DSC reported in this work.

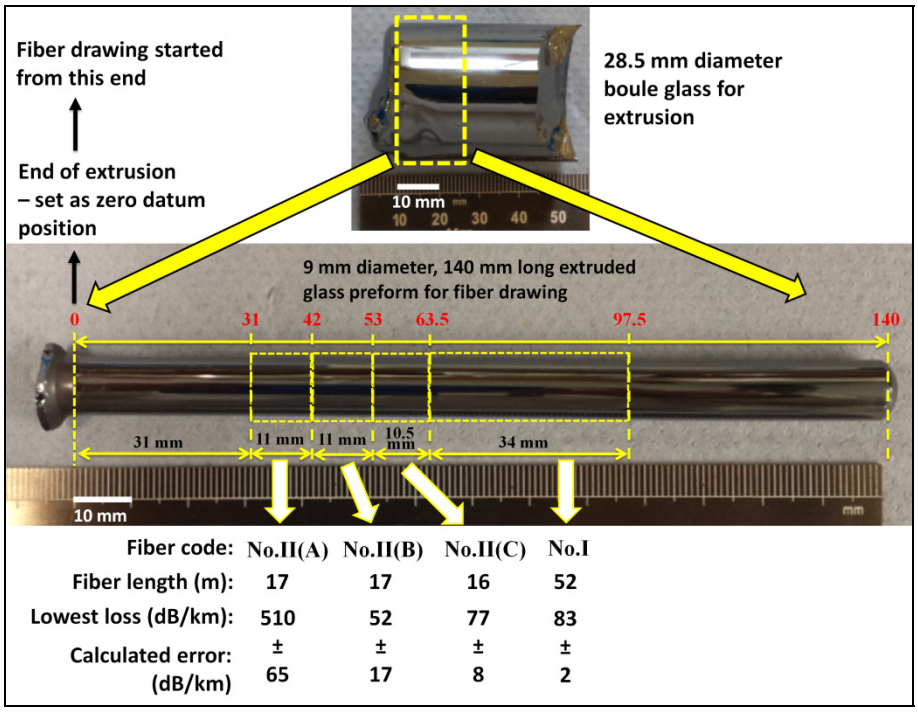

Fig. 1. As-annealed $Ge_{10}As_{21}Se_{69}$ (at%) boule glass (diameter = 28.5 mm) and the extruded 9 mm diameter unclad. preform. The preform was drawn into fibers (*i.e.* code: No.I, No.II(A), No.II (B) and No.II (C)) and the corresponding positions of the preform are shown. The fiber loss spectra are presented in Fig. 8 and Fig. 9.

#239909 Received 28 Apr 2015; revised 22 May 2015; accepted 15 Jun 2015; published 7 Jul 2015

In the fiber preform preparation, Ge (5N purity, Materion), As (7N5 purity, Furakawa Denshi; prior heat treated at 310°C under vacuum (10^{-3} Pa)), Se (prior purified by distillation at ~450°C under vacuum (10^{-3} Pa), from a source of 5N purity, Materion), 1000 ppmw $TeCl_4$ (3N purity, Alfa Aesar; used as a [H] getter) and 750 ppmw Al (6N purity, Alfa Aesar; used as an [O] getter) were batched (nominal composition of $Ge_{10}As_{21}Se_{69}$) and melted (12 hours at 850°C) in a silica glass rig and experienced double distillation at ~750°C under vacuum (10^{-3} Pa). After distillation, the glass was melted (10 hours at 800°C), air quenched to T_g and annealed at T_g for ~1 hour and cooled down to ambient temperature. The as-annealed glass boule was 50 mm long and of 28.5 mm diameter (see Fig. 1). Then the boule glass was extruded into a 140 mm long, 9 mm diameter glass preform (see Fig. 1) with a *ca.* 2.8 mm/min. extruding rate using an in-house extruder (see [35] for more details of the extruder); the extruded preform was axially straight. Finally, the preform was drawn into >100 meters long, 235 ± 5 μm diameter unstructured (*i.e.* unclad.) fiber with a drawing rate of 4.6 m/min. by means of a radio frequency fiber-drawing furnace on a customized Heathway fiber-drawing tower. In this work, four parts of the fiber, coded No.I, No.II(A), No.II(B) and No.II(C) underwent optical attenuation measurement (total length of all fiber tested > 100 meters); the corresponding position on the preform of each fiber part was calculated and is shown in Fig. 1.

2.2 Bulk glass and fiber characterization

2.2.1 Bulk glass characterization: viscosity-temperature and DSC

In the viscosity-temperature measurements, a Perkin Elmer TMA7 thermomechanical analyzer (TMA) and a parallel-plate method [41] were used. 4.1 mm diameter TMA viscosity disc samples were prepared from a glass remelt (2 hours at 850°C). The samples were either 1.6 mm or 4.1 mm in height, corresponding to a 70 mN or a 420 mN applied constant load in the TMA measurement, respectively, in order to access different viscosity-temperature ranges. In the measurement, the isochronal heating rate was 2.5-10°C/min up to ~100-200°C above T_g under flowing He. The estimated error was no more than ± 2°C on the temperature values and $\sim 10^{\pm 0.05}$ Pa.s on the viscosity values.

DSC measurement was carried out in a Perkin Elmer Pyris1 Differential Scanning Calorimeter by using an isochronal heating/cooling rate of 10°C/min, under flowing Ar. Close to 20.5 mg of the as-prepared (no prior remelt) chalcogenide glass chunks were sealed inside an Al pan as the DSC sample, with an empty pan as the reference. For checking the reproducibility, the DSC sample was first heated twice through a cycle, comprised of heating to ~T_g + 50°C (*i.e.* ~210°C) and cooling to 40°C, and finally heated up through T_g to ~300°C, *i.e.* the sample went through T_g three times. T_g was obtained by constructing the intersection of the extrapolated onset of the maximum gradient of endothermic peak with the pre-T_g baseline, to an accuracy of ± 2°C.

2.2.2 Fiber loss measurement and loss error

A Fourier transform infrared (FTIR) spectrometer (Bruker IFS 66/S) was engaged in developing the robust methodology of cut-back loss-measurement in this work. Due to the difficulty in producing good quality cleaves in non-silica-based optical fibers, and in order to get reliable and reproducible results, a 'group-cleave' process was developed and used to identify the best cleaves amongst the good cleaves. This approach was taken in an endeavor to remove, or at least minimize, the effect of the cleave itself, on the loss measurements. The fiber loss spectrum then better reflects the fiber material quality, and geometrical quality, rather than reflecting spurious loss artifacts introduced by the cleaving process.

The equation for calculating the fiber optical loss is given in Eq. (1).

$$Loss(dB/m) = -(10/L)\cdot \log_{10}(P_{out}/P_{in}) \quad (1)$$

#239909 Received 28 Apr 2015; revised 22 May 2015; accepted 15 Jun 2015; published 7 Jul 2015

where L is the length of fiber removed by cut-back between two cleaves at which the measured optical power is P_{out} before cutting back and P_{in} after cutting back. P_{out} and P_{in} are optical power spectra and the calculation in Eq. (1) is performed at each wavelength in the range considered.

Figure 2(a) shows a sketch of the glass fiber loss measurement, with two groups of cleaves. A group of cleaves was made at the exit end of the fiber under test and an optical power spectrum was recorded from each cleave, the lengths of fiber removed for each cleave were kept to a minimum and were recorded, this group was designated "group one". Next an appropriately longer length of fiber was removed, length recorded, and another group of cleaves was made as before with an optical power spectrum being recorded for each cleave in this "group two". Taking the spectrum for any cleave from group one (P_{out}) and any cleave from group two (P_{in}), the loss could be calculated using Eq. (1). In this method, there were typically (down to manual skill) about three good cleaves in each group. However to ensure that only the best cleaves were used to determine fiber loss, the following method was applied.

(i) Taking a (any) cleave from group one (*i.e.* P_{out} was fixed), the loss spectrum was individually calculated for each cleave in group two (P_{in}). The best quality cleave in group two would show the highest optical power, hence P_{in} would be greatest and the loss was calculated to be the greatest (using Eq. (1)). Thus the highest loss calculated using Eq. (1) corresponded to the best cleave in the cleave group two.

(ii) An optical power spectrum of any cleave from group two was used (i.e. P_{in} was fixed) to calculate fiber loss for each of the cleaves in group one (P_{out}). In this case the best cleave in group one, giving the greatest P_{out} corresponded to the lowest loss spectrum (see Eq. (1)). Thus the lowest loss was deemed to be associated with the best cleave in the cleave group one.

(iii) At the end, the best cleave pair from both groups, given by this method, were used for calculating the final fiber optical loss spectrum.

The method described above was engaged in the measurement of the No.I fiber (see Fig. 2(a)) and 52 meters of No.I fiber were used in total. In No.I fiber, group one cleaves were named 1a, 1b and 1c, respectively (see Fig. 2(a)). A 49 m long fiber was cut between cleaves of groups one and two. The group two cleaves were named 2a, 2b and 2c, respectively (see Fig. 2(a)). Optical micrographs presented in Fig. 3 show the quality of all the cleaves used in the loss measurement of the No.I fiber. The calculated best cleaves 1c and 2b of Fig. 3 were used for the calculation of the loss spectrum of the No.I fiber, which is shown in section 3.2.

Figure 2(b) shows a sketch of the loss measurement for the No.II(A), No.II(B) and No.II(C) fibers, which were of 50 meters' total length; this total piece of fiber is referred to as 'No.II fiber' here. The position of the preform that was used to draw the No.II fibers was closer to the end part of the extrusion (*i.e.* the last part of the extrudate to leave the die) than the No.I fiber, with a concomitant greater risk of more impurity in the No.II fibers. Therefore, in the loss measurement, the No.II fibers were designed to have four groups of cleaves, instead of the two groups of cleaves that were normally applied, and this could help examine if any particular piece of the fiber had higher loss. In line with the same method as has already been introduced above for the No.I fiber, here one best cleave was identified in each of the four groups and the optical micrographs of these 'best' cleaves are shown in Fig. 4. Finally, the optical loss spectra of the fibers of No.II(A), No.II(B) and No.II(C), were calculated using the best cleaves in the adjacent groups: one&two, two&three and three&four, respectively.

As a final comment on our methods, in measuring the fiber optical attenuation of $Ge_{10}As_{21}Se_{69}$ (at%) fiber, our two slightly differing approaches described here for the No.I and No.II fibers are illustrative of our generic, careful approach in which we wish to understand and shed greater light on our fiber optical quality.

#239909 Received 28 Apr 2015; revised 22 May 2015; accepted 15 Jun 2015; published 7 Jul 2015

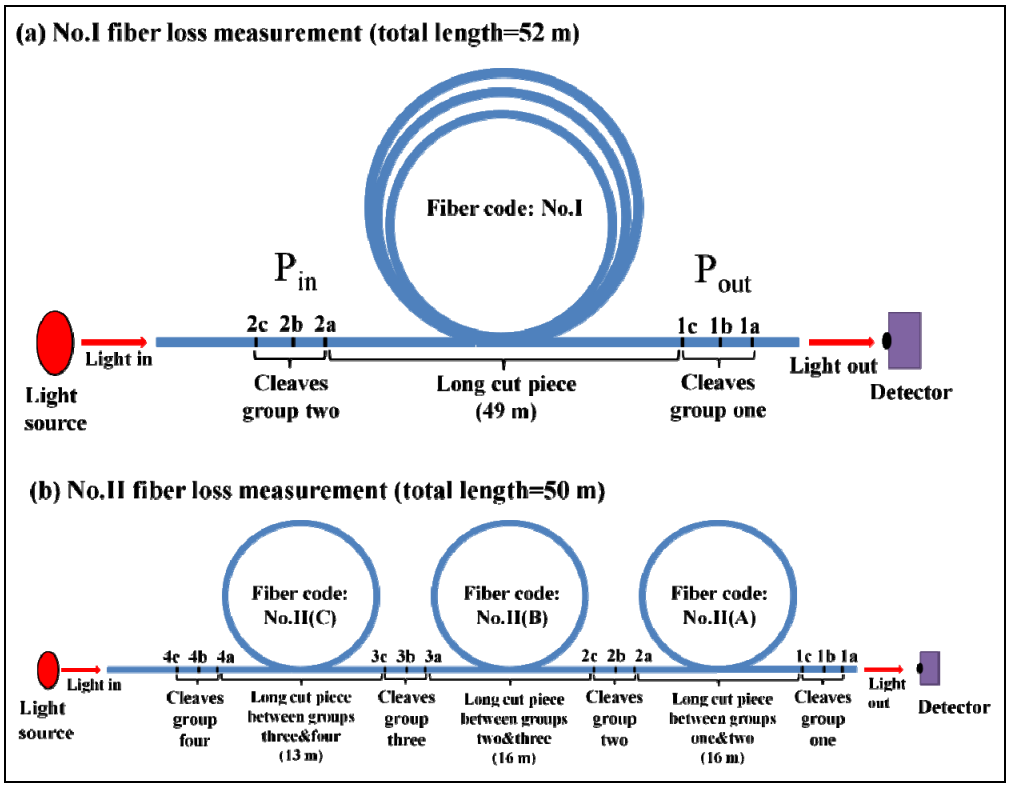

Fig. 2. Sketch of the developed fiber loss measurements applied in this work shown here for the $Ge_{10}As_{21}Se_{69}$ (at%) fiber, comprising the No.I fiber and the No.II fibers (consisting of the No.II(A), the No.II(B) and the No.II(C) fibers). As depicted in the figure part (a), there were: 52 meters of the No.I fiber and two groups of cleaves for the No.I fiber, namely: group one (1a, 1b, 1c) and group two (2a, 2b, 2c) cleaves in the loss measurement of the No.I fiber. Similarly, as depicted in the figure part (b), there were 50 meters in total of the No.II fibers (comprising the No.II(A), the No.II(B) and the No.II(C) fibers) and four groups of cleaves (namely: group one (1a, 1b, 1c), group two (2a, 2b, 2c), group three (3a, 3b, 3c) and group four (4a, 4b, 4c)) in the loss measurements for the No.II fibers (comprising the No.II(A), the No.II(B) and the No.II(C) fibers). P is optical power spectrum.

The loss error/deviation in a fiber loss measurement can be affected by factors like cleaving quality, which is often the main issue, fiber diameter deviation and the stability of the optical system *etc.*. The fiber lengths used when measuring low loss fiber are generally from > 5-10 m [8, 18, 42] and up to 100 m [2, 43]. In a loss measurement scheme, provided there is still sufficient power collected from the output of the fiber to ensure a reasonable signal-to-noise ratio at the detector, then using as long a piece of fiber as possible helps reduce the loss error in a fiber loss measurement because then the measured light power at the fiber exit-end is affected mainly by the fiber material quality and fiber physical quality, (deviations from perfect fiber geometry and perfect glass interfaces raise the measured loss) instead of the cleaving quality itself. In other words, the difference between P_{in} and P_{out} in Eq. (1) is dominated by fiber loss and not by the cleaves.

The cleaving process relies on conchoidal fracture, typical of glassy materials, and is especially vulnerable to problems in these low Young's modulus, non-silica glasses. The original crack-defect, added on purpose at the fiber surface to start the cleave of the fiber, under fiber tension grows across the fiber to give mirror, mist and, possibly, hackle regions, moving out from the original defect. As evidenced in Figs. 3 and 4, the best cleaves are perpendicular to the fiber axis and leave behind only the original imposed defect, a

#239909 Received 28 Apr 2015; revised 22 May 2015; accepted 15 Jun 2015; published 7 Jul 2015

dominating mirror region and possibly just the start of mist where the propagating fracture energy hits, and maybe is reflected from another fiber edge (often opposite from the edge location of the original defect).

For a step-index, core/clad. fiber, the core guiding region, where the light is propagating, might reasonably be expected to be much less affected by the unavoidable residual edge defect, which was the original defect of the cleaving process, in the cleaved cross-section of the fiber. However, the internal core/clad. glass interfaces may arrest the crack propagation and cause cleave discontinuity and light scattering. This would be especially true if thermal stress mismatch, due to differing thermal expansion coefficients below T_g, exists between the core and cladding glasses used, or if any permanent stress is left in the fiber, after forming the fiber and cooling to ambient, arising from differing T_gs of the component glasses making up the fiber. For an unclad fiber (*i.e.* single-index), where light propagates across the whole cross-section, the loss error can be affected more by the cleaving quality as the original defect, purposefully made, unavoidably sits in the light-guiding region. The error in determination of chalcogenide glass fiber optical losses has been estimated to be around ± 4% at the 1000 dB/km level and ± 8% at the 100 dB/km level, for both unclad [18]. and core/clad [42–44]. fibers.

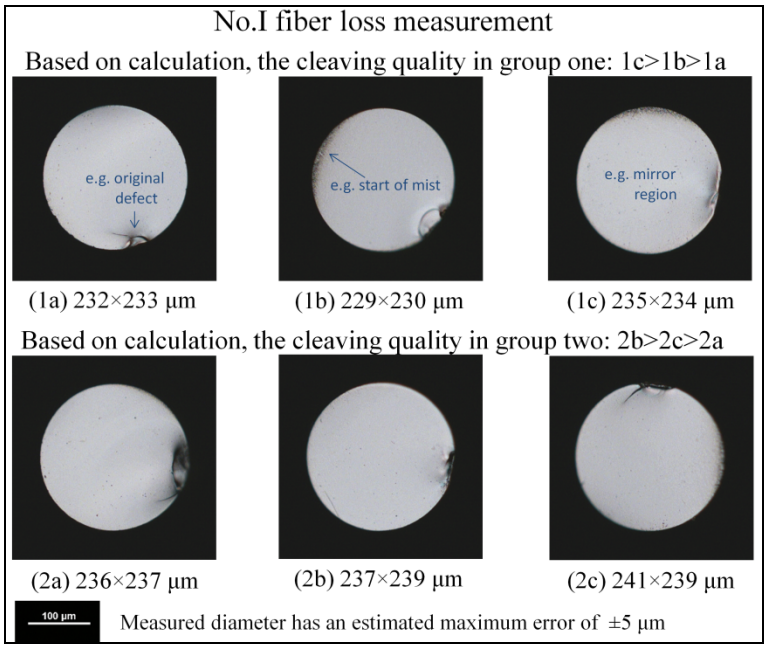

Fig. 3. Optical micrographs of the cleaves applied in the loss measurement of the No.I fiber of $Ge_{10}As_{21}Se_{69}$ (at%) glass. The optical loss spectrum of the No.I fiber in Fig. 8 was calculated using the two best cleaves in group one (*i.e.* 1c) and group two (*i.e.* 2b). The measured loss error/standard deviation of the optical loss spectrum of the No.I fiber was achieved based on cross-calculation of cleaves between group one, and group two, cleaves and is given in Table 2.

#239909 Received 28 Apr 2015; revised 22 May 2015; accepted 15 Jun 2015; published 7 Jul 2015

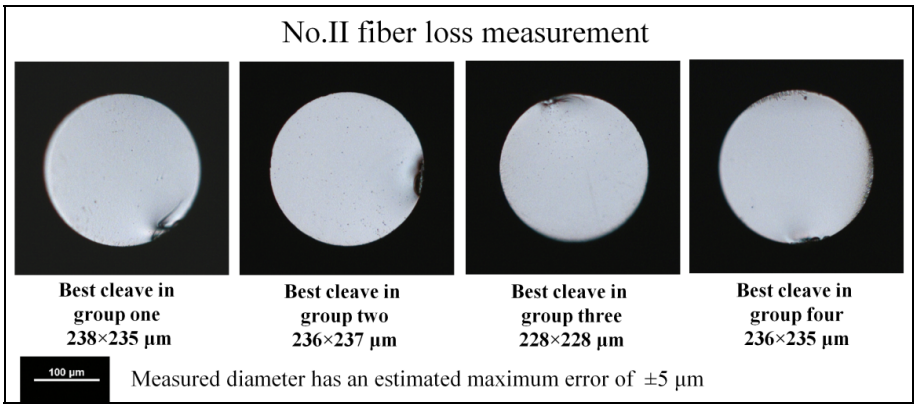

Fig. 4. Optical micrographs of the best cleaves achieved in each of the four groups of optical loss measurement of the No.II fibers of $Ge_{10}As_{21}Se_{69}$ *viz.*: No.II(A), No.II(B) and No.II(C). Optical loss spectra of the No.II (A), the No.II (B) and the No.II (C) fibers presented in Fig. 9 are based on the calculation of the best cleaves between each of the adjacent groups one&two, two&three and three&four, respectively.

In this work, for calculation of a loss-spectrum, two groups of good cleaves were used and the loss error of the measurement was evaluated by the standard deviation of the loss results by cross-calculation of all cleaves between the two groups. Table 2 shows the calculated results of loss error in the loss measurement of the No.I fiber. In this calculation, the wavelengths: 2.7092 µm and 3.8500 µm were selected because the No.I fiber spectrum had low loss and was smoothly varying, with no obvious absorption band present, at these wavelengths and we concluded that loss here was probably affected only by intrinsic and extrinsic scattering, rather than by absorption. Because there were three (good) cleaves in each of the two groups, there were nine calculated loss results in total at each wavelength for the No.I fiber. The cleaving quality of these cleaves can be found in Fig. 3. The calculated standard deviation of the loss measurements was 2 dB/km at both wavelengths of 2.7092 µm and 3.8500 µm, and this was taken as the error on the optical loss of the No.I fiber. Thus, by using this developed cut-back method, we suggest that the loss error can be improved to be ± 2% at the 100 dB/km level loss (see Table 2).

Table 2. Error/standard deviation calculation on the loss measurement of the No.I fiber. 2.7092 µm wavelength and 3.8500 µm wavelengths were chosen because the fiber spectrum exhibited low loss and was smoothly varying at both these wavelengths and probably was affected only by extrinsic and intrinsic scattering, rather than absorption. In the Table, as an example, for convenience, *'1a-2a'* is the notation taken for the calculation of loss between cleave 1a and cleave 2a. Cleave quality for the No.I fiber is in Fig. 3. The optical loss spectrum of the No.I fiber may be found in Fig. 8 and was calculated using the two best cleaves: 1c and 2b.

	At 2.7092 µm wavelength			At 3.8500 µm wavelength		
Cleaves	*1a-2a*	*1a-2b*	*1a-2c*	*1a-2a*	*1a-2b*	*1a-2c*
Loss / (dB/km)	172.0	175.6	175.1	140.1	143.3	142.1
Cleaves	*1b-2a*	*1b-2b*	*1b-2c*	*1b-2a*	*1b-2b*	*1b-2c*
Loss / (dB/km)	170.7	174.4	173.9	138.7	141.9	140.8
Cleaves	*1c-2a*	*1c-2b*	*1c-2c*	*1c-2a*	*1c-2b*	*1c-2c*
Loss / (dB/km)	170.2	174.0	173.5	137.0	140.3	139.2
Calculated standard deviation / (dB/km)		1.9			1.9	

By the same error calculation method, the calculated errors for the loss of the No.II(A), No.II(B) and No.II(C) fibers were 65 dB/km, 17 dB/km and 8 dB/km, respectively, by the

#239909 Received 28 Apr 2015; revised 22 May 2015; accepted 15 Jun 2015; published 7 Jul 2015

cross-calculation made between the adjacent cleaving groups, *i.e.* groups one&two, two&three, three&four, respectively, see Fig. 2(b). Measurement of the No.I fiber showed the lowest loss error (2 dB/km), not only because the No.I fiber had comparatively better quality of all the six cleaves in both groups but also because the No.I fiber had the longest length (52 m; long-cut-piece had length of 49 m) of fiber in the measurement (*cf.* long-cut-pieces of the No.II(A), No.II(B) and No.II(C) were of lengths: 16 m, 16 m and 13 m, respectively, see Fig. 2) and thus a lower error was achieved. Please note that the actual errors could be even smaller than the calculated errors presented here; this is because only the best cleaves were applied in the calculation for presenting the final loss spectrum, but for the error calculation, then cleaves which were not as good as the best cleaves were also used. Finally, please note, in an extreme case, if the diameter of a fiber has small variation in each cleave group but has a big variation between two cleave groups (*e.g.* a tapered fiber), the calculated loss error can be small but the measured loss does not reflect the real loss of a "uniform" fiber.

3. Results and discussion

3.1 Thermal properties

Figure 5 presents the viscosity-temperature curves of the $Ge_{10}As_{21}Se_{69}$ (at%) supercooled glass melt collected at 10°C/min. From Fig. 5, it may be seen that the supercooled glass melt has a typical extrusion viscosity of $10^{8.0}$ Pa.s at 218°C and a typical fiber-drawing viscosity of $10^{4.5}$ Pa.s at 311°C. According to Fig. 5, for isoviscous points, the viscosity-temperature curves in both the lower viscosity region (sample size: 1.6 mm, load 70 mN) and the higher viscosity region (sample size: 4.1 mm, load 420 mN) exhibit an error/standard deviation which is well within the estimated 2°C errors given above (section 2.2.1).

Figure 6 shows the viscosity-temperature curves obtained using different isochronal heating rates from 2.5°C/min to 10°C/min (same sample height 4.1 mm and load 420 mN). It is suggested that, because of the time-lag of heat transfer to the rod samples, the viscosity-temperature curves have tended to shift to a higher temperature when the heating rate was greater. However, this shift is rather small, *e.g.* $< 10^{0.2}$ Pa.s at any fixed temperature. In this work, the $Ge_{10}As_{21}Se_{69}$ supercooled glass melt tended to a steady-state extrusion rate at 212°C corresponding to a viscosity of $10^{8.1\text{-}8.3}$ Pa.s, according to the viscosity-temperature curves in Fig. 6.

The DSC curves of $Ge_{10}As_{21}Se_{69}$ are presented in Fig. 7. In the DSC measurement, the sample was taken through T_g three times to check the T_g reproducibility, because the glass T_g will have been affected by the glass thermal history. When the glass sample in the DSC equipment went through the T_g region for the first time then the glass thermal history was the air-quenching, followed by full annealing, that had taken place during the glass manufacture. This annealing comprised an isothermal hold at T_g for 1 hour, the furnace was then switched off with the glass melt *in situ* and allowed to cool naturally without forced cooling. For this thermal history the DSC T_g value was 161°C. On the other hand, for both the second and the third times of passing through the T_g region, the thermal history of the glass sample was the same and comprised a quenching *in situ* to ambient inside the DSC at a rate of 10°C/min with no specific annealing schedule applied. Therefore, as might be expected, for the second and third times of passing T_g, the glass T_gs were the same: 158°C with a standard deviation of < 2°C, which is comparable to other work [45]. Also, no distinct crystallization peak was observed during these DSC runs, in particularly in the temperature regime used for the extrusion (212°C-218°C, see Fig. 6).

#239909 Received 28 Apr 2015; revised 22 May 2015; accepted 15 Jun 2015; published 7 Jul 2015

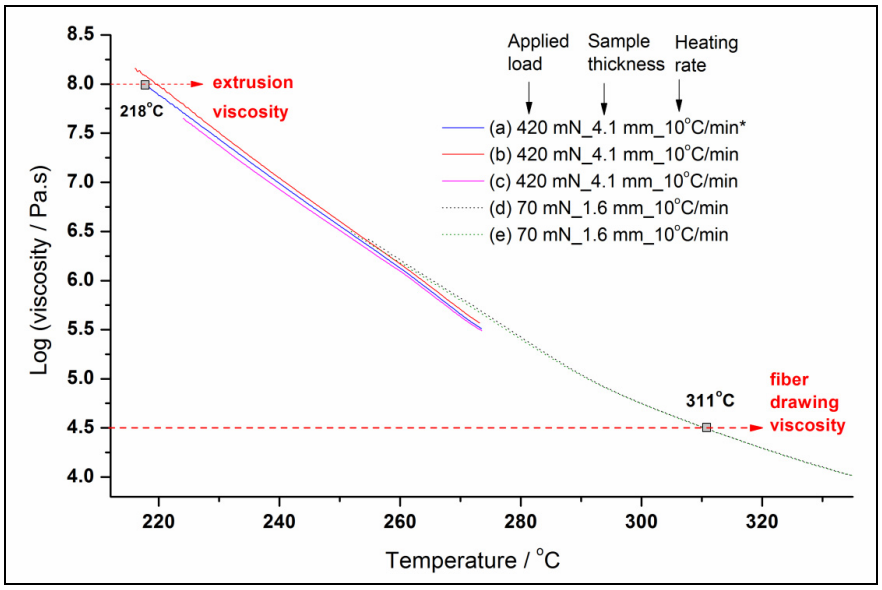

Fig. 5. Viscosity-temperature curves of the $Ge_{10}As_{21}Se_{69}$ supercooled glass melt collected at 10°C/min. Solid curves are for the 4.1 mm thick glass samples that could achieve comparatively high viscosity ($10^{8.0}$ Pa.s); dotted curves are for the 1.6 mm thin glass samples that could achieve comparatively low viscosity ($10^{4.5}$ Pa.s). In this way the full viscosity/temperature range of interest could be covered.

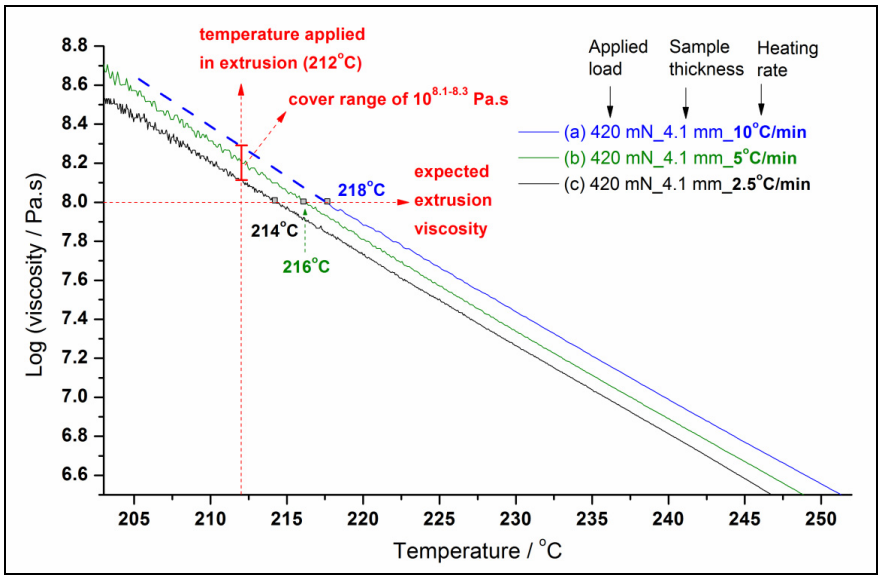

Fig. 6. Viscosity-temperature curves of the $Ge_{10}As_{21}Se_{69}$ supercooled glass melt using isochronal heating rates of: (a) 2.5°C/min, (b) 5°C/min and (c) 10°C/min, from the lower black curve to the upper blue curve, respectively. The blue viscosity-temperature curve (a), here in Fig. 6, was the same sample and is the same viscosity-temperature curve as curve (a) in Fig. 5.

#239909 Received 28 Apr 2015; revised 22 May 2015; accepted 15 Jun 2015; published 7 Jul 2015

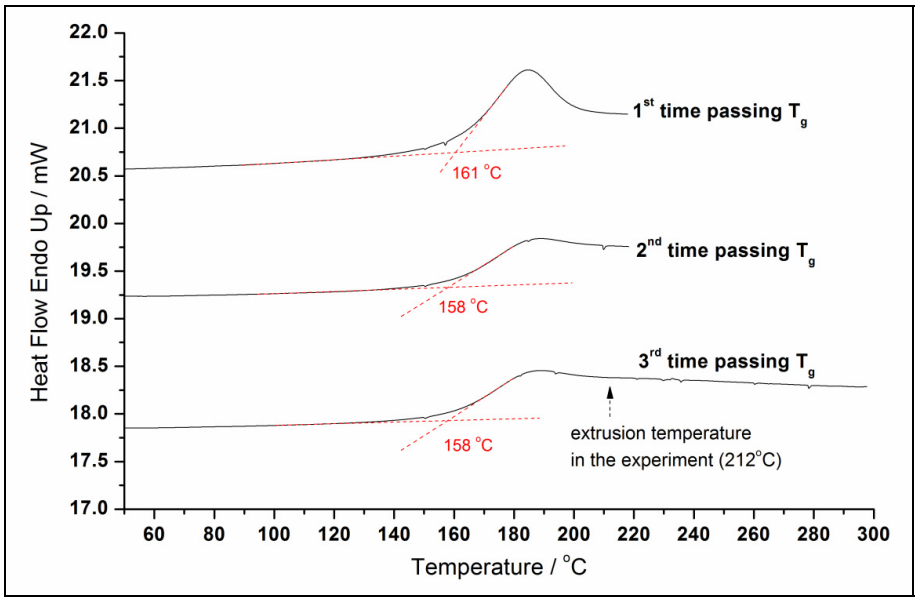

Fig. 7. DSC curves of the as-annealed $Ge_{10}As_{21}Se_{69}$ glass (heating rate: 10°C/min). From top to bottom, T_gs are shown for the glass sample that passed through T_g once, twice and thrice. Note that the upper DSC curve shows a different T_g because the thermal history of the glass sample was different, whereas the two lower DSC curves show the same T_g and the sample in both cases had the same thermal history. The extrusion temperature as labelled on the DSC curve is the actual one used in the extrusion experiment. The tiny blips in the DSC curves arose from adventitious mechanical vibration during the measurement.

3.2 Optical fiber loss

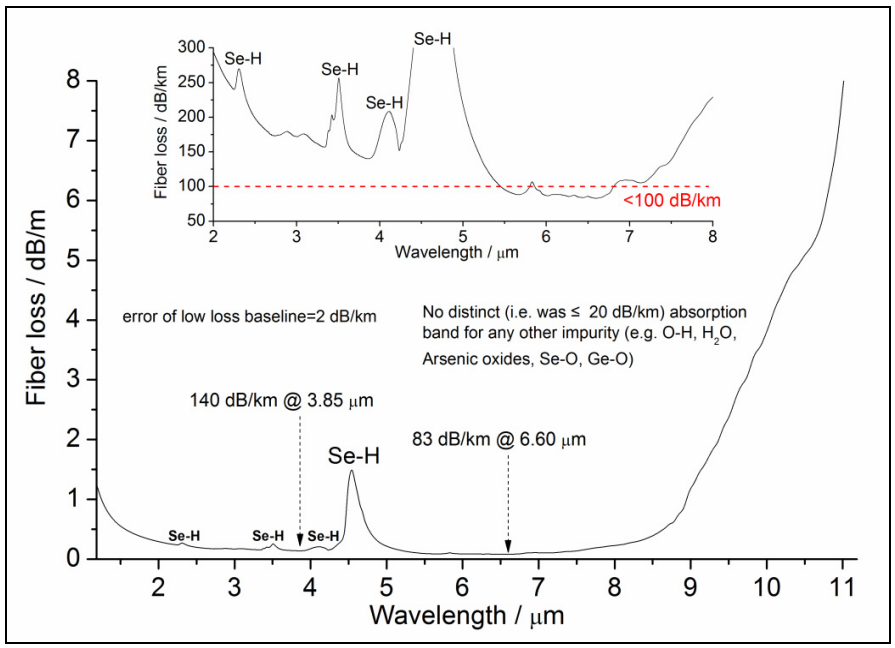

Fig. 8. Optical loss spectrum of the unclad. $Ge_{10}As_{21}Se_{69}$ No.I fiber. Inset shows more clearly the sub-100 dB/km loss characteristic. The corresponding position of the preform used in fabricating the No.I fiber can be found in Fig. 1. Optical micrographs of the two best fiber cleaves used in the loss calculation of the unclad. $Ge_{10}As_{21}Se_{69}$ No.I fiber are in Fig. 3.

#239909 Received 28 Apr 2015; revised 22 May 2015; accepted 15 Jun 2015; published 7 Jul 2015

Figure 8 shows the optical loss spectrum of the No. I fiber of $Ge_{10}As_{21}Se_{69}$ glass, and covers the spectral wavelength range of 1.3-11 μm. Because 52 meters of the No.I fiber were taken for the loss measurement and good cleaves were used, the error was only 2 dB/km. Hence, we have taken the No.I fiber loss as the standard fiber loss result of this work. From Fig. 8, the lowest loss was 83 dB/km at 6.6 μm wavelength, whilst the loss was 140 dB/km at 3.85 μm wavelength. The baseline was 83-90 dB/km across the 5.6-6.8 μm wavelength region, which was lower than the baseline of 140-190 dB/km across the 2.6-3.9 wavelength region. The loss rose with increasing photon energy below 2 μm wavelength; this was mainly due to the onset of the optical bandgap and in particular to the weak absorption tail [20]. However, a reciprocal wavelength dependent scattering may also have contributed in this region. This could have been Mie or Rayleigh-Gans extrinsic scattering, due to larger scattering centers of a size which may have approached the wavelength of the light, as well as the underlying Rayleigh scattering - an intrinsic loss mechanism arising from tiny micro-compositional/micro-density fluctuations '*frozen- in*' at T_g during cooling of the supercooled glass melt to make glass.

From the No.I fiber spectrum shown in Fig. 8, the only clear impurity is Se-H, which is known to exhibit vibrational absorption bands at wavelengths of 2.3 μm (weak), 3.5 μm (weak), 4.1 μm (weak) and 4.5 μm (strong) [[46]]. The latter displayed 1.4 dB/m at 4.5 μm wavelength, corresponding to a concentration of 1.27 ppm(at.) H in the form of Se-H (or 0.016 ppmw H in the form of Se-H), using the extinction coefficient: 1.1 dB/m/ppm(at.) for Se-H at 4.5 μm (validated value from private communication, V. Shiryaev (2015), after [[7, 15]]). No distinct (i.e. was ≤ 20 dB/km) absorption band is seen in Fig. 8 for any other impurity: implying no distinct O-H band at 2.9 μm wavelength [[12]], no distinct H_2O band at 6.3 μm wavelength [[46]] nor distinct oxide impurity bands at > 7.5 μm wavelength (i.e. no [= As-O], [-Se-O], [≡Ge-O] and [≡Si-O]) [[47, 48]]. From Fig. 8, the loss was 1.20 dB/m at 9 μm wavelength, increasing to 3.85 dB/m at 10 μm wavelength and 7.70 dB/m at 11 μm wavelength; the post-10μm-wavelength losses may have been due to overtone and combination vibrational absorption bands of the fundamental stretching, anti-stretching and bending absorption bands due to ≡Ge-Se, = As-Se, = As-Se-As = and ≡Ge-Se-Ge≡ and = As-Se-Ge≡ structural units, analogous to the overtone and combination bands reported at ≥ 10 μm wavelength in $As_{40}Se_{60}$ glasses as discussed by the group of Moynihan [49]. In summary, the loss spectrum of the $Ge_{10}As_{21}Se_{69}$ glass No.I fiber presented a minimum baseline loss of 83 ± 2 dB/km, superposed by 1.4 dB/m loss at 4.5 μm (Se-H impurity) and no other distinct impurity bands (*viz.:* O-H, As-O and Ge-O and SiO_2). To our knowledge, this is the lowest loss to date for Ge-As-Se glass fiber, with regard to minimum loss, baseline loss and absence of impurity vibrational absorption bands. The inset of Fig. 8 depicts the sub-100 dB/km spectral region.

Figure 9 compares optical loss spectra of the $Ge_{10}As_{21}Se_{69}$ glass fibers that came from different positions of the extruded preform (see Fig. 1), as follows: the No.II(A) fiber, the No.II(B) fiber, the No.II(C) fiber and the No.I fiber came from the preform positions 31-42 mm, 42-53 mm, 53-63.5 mm and 63.5-97.5 mm, respectively, where the end of extruded preform (that is the last part of the extrudate to have emerged from the extruder die) was taken as the zero millimeter datum position; see Fig. 1.

From Fig. 9, the lowest optical attenuation of the $Ge_{10}As_{21}Se_{69}$ glass No.II (A) fiber, No.II (B) fiber, No.II (C) fiber and No.I fiber are all at 6.6 μm wavelength and are: 510 ± 65 dB/km, 52 ± 17 dB/km, 77 ± 8 dB/km and 83 ± 2 dB/km, respectively. Please note that although the $Ge_{10}As_{21}Se_{69}$ glass No.II (B) fiber exhibited the lowest loss (52 dB/km), its loss error (17 dB/km) was larger than the loss errors in No.II (C) and No.I fibers which were 7 dB/km and 2 dB/km, respectively.

#239909 Received 28 Apr 2015; revised 22 May 2015; accepted 15 Jun 2015; published 7 Jul 2015

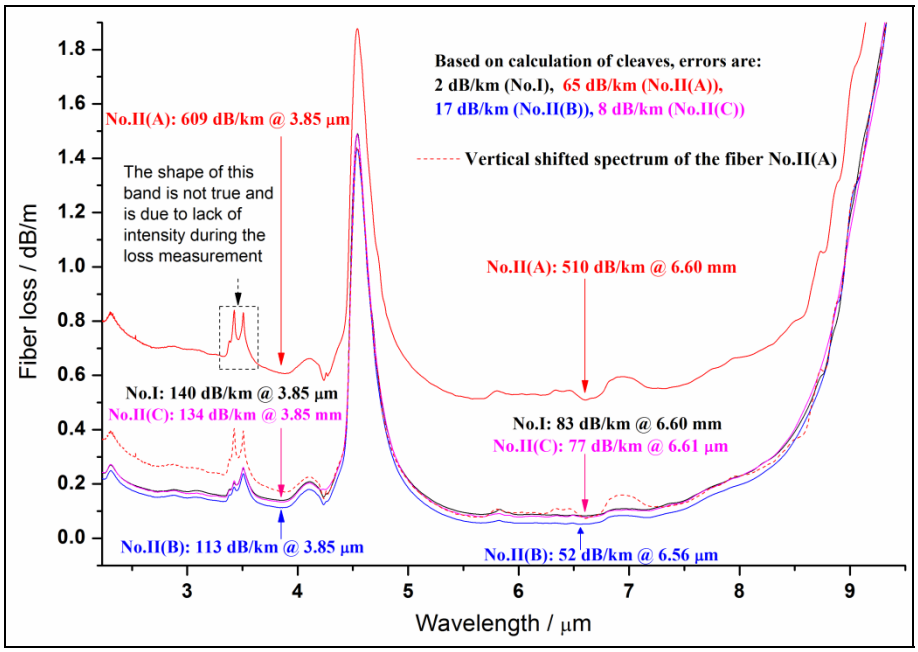

Fig. 9. Optical loss comparison of the spectra of the No.I, No.II(A), No.II(B) and No.II(C) fibers (unclad. fiber of nominal composition $Ge_{10}As_{21}Se_{69}$ (at%)). For convenience, the dotted line is the vertically shifted spectrum of the No.II(A) fiber for comparison of its extra absorption and scattering loss. The preform position from which each fiber originated is given in Fig. 1. Optical micrographs of the best fiber cleaves used in the calculation of the spectral loss here are presented in Fig. 3 and Fig. 4.

On the one hand, Fig. 9 presents spectra of No.II(B), No.II(C) and No.I fibers which had been adjacent to each other in the preform (position: 42-97.5 mm, see Fig. 1) showing similar loss; the small difference was partly caused by the material and partly due to the loss error caused by the cleave quality and fiber length used in the loss measurement (see section 2.2.2). These similar loss results indicate good stability of the glass material and the reproducibility of the fiber loss measurement.

On the other hand, the No.II(A) fiber which was from the last part of the preform to emerge from the extrusion die had the highest minimum loss of 510 ± 65 dB/km amongst the four fiber spectra in Fig. 9. Moreover, the baseline loss of the No.II(A) fiber was far higher (500-700 dB/km over 3-7.5 μm wavelength) than that of the No.II(B), No.II(C) and No.I fibers (50-180 dB/km, over 3-7.5 μm wavelength). Also in Fig. 9, comparing all fibers, the dotted, vertically-shifted spectrum of the $Ge_{10}As_{21}Se_{69}$ glass No.II(A) fiber showed extra scattering loss below 4 μm wavelength.

To summarize, the No.II(A) fiber which was closer to the end of the extruded material (preform position: 31-42 mm, see Fig. 1) had emphatically the highest spectral loss. This is suggested to have been caused mainly by impurities accumulating in the end part of the extrudate. Thus, by the end of the extrusion, the bulk of the boule glass charge had been extruded and gone on to form low loss fiber but the remaining boule glass extruder charge, we suggest, had more time in the extruder and more physical contact with the metal inside the extruder barrel, leading to imbibition of metallic impurities causing wavelength-independent scattering loss and also some finer particles causing Mie and/or Rayleigh-Gans scattering loss up to ~4 μm wavelength [50]. Our previous work [35] on Ge-As-Se/Ge-As-Se-S core/clad. co-extruded preforms, also showed deterioration of the last part of the extrudate. Defects at the core/clad. interface, were found to be maximized near the start of the co-extrusion, but these were mainly due to gas entrapment bubbles at the point of mating of the core/clad glass

#239909 Received 28 Apr 2015; revised 22 May 2015; accepted 15 Jun 2015; published 7 Jul 2015

surfaces during the extrusion. There followed a negligible defect population in the middle of the co-extruded preform. The defect population was found to rise towards the end of the extrudate, as found here, and this possibly also was due to unwanted, metallic *etc.* impurities imbibed in to the supercooled glass melt as it flowed in contact with the internal extruder surfaces. An additional reason for such a distinction of loss increase could be crystallization; the end of the extrudate had a longer time in the extruder and such metallic impurities could act as nucleation agents.

4. Summary

In this work, we report the lowest loss Ge-As-Se chalcogenide glass fiber ($Ge_{10}As_{21}Se_{69}$ (at%) obtained to date, to our knowledge, achieving 83 dB/km at 6.60 μm wavelength, with a calculated error of 2 dB/km. Furthermore, light was collected and measured after having traversed along 52 m of the fiber. The background fiber loss was 83-90 dB/km at 5.6-6.8 μm and 140-190 dB/km at 2.6-3.9 μm with a superposed impurity absorption due to 1.27 ppm(at.) H in the form of Se-H giving 1.4 dB/m loss at 4.5 μm wavelength but with no other distinct (*i.e.* was ≤ 20 dB/km) impurity bands of -O-H, H_2O, = As-O, ≡Ge-O, ≡Si-O and -Se-O-. The glass was purified by double distillation with getters and then extruded prior to fiber-drawing. Pertinent to the preform and fiber manufacture, the viscosity-temperature curves and DSC curves of the $Ge_{10}As_{21}Se_{69}$ glass were reported. Best practice methodology for these measurements and for measuring fiber optical loss and calculation of loss error/deviation was presented. Fiber loss variation with extruded preform position was reported. The reliable lowest loss was found for fiber drawn from a mid-position of the extruded preform. For fiber drawn from more than about 40 mm from the end of preform (*i.e.* 4 cm from the end of the extrusion), optical loss was similar to the best low loss, and minimum losses for fiber drawn from positions along the extruded preform were: 52 ± 17 dB/km, 77 ± 8 dB/km and 83 ± 2 dB/km which indicates good glass stability of the material. However, fiber drawn from the end of the preform (that extruded last from the extruder die) manifested a large increase in minimum loss to 510 ± 65 dB/km. This, together with extra NIR scattering loss, implied that the last part of the glass extrudate had had most contact with the extruder internal surfaces and had gathered contaminants like metallic particles and/or crystallization occurred.

Acknowledgments

This research was supported by the European Commission through Framework Seven (FP7) project MINERVA MId- to NEaR infrared spectroscopy for impro**V**ed medical the di**A**gnostics (317803; www.minerva-project.eu). We particularly acknowledge the MINERVA support, for Prof. Vladimir S. Shiryaev, which directly enabled international cooperation to take place at the University of Nottingham, UK.

#239909 Received 28 Apr 2015; revised 22 May 2015; accepted 15 Jun 2015; published 7 Jul 2015